Temperature dependence of uniaxial magnetic anisotropy constants and spin-reorientation transition in the single-ion one-sublattice system

Yu Ming-hui and Zhang Zhi-dong
Institute of Metal Research, Chinese Academy of Sciences, Shenyang 110015, People's Republic of China
and International Center for Materials Physics, Chinese Academy of Sciences, Shenyang 110015, People's Republic of China
(Received 31 March 1999)

Based on an effective parameter method in the mean-field approximation, the temperature dependence of the single-ion anisotropy constants in the uniaxial one-sublattice system has been exhaustively studied within the three-constant approximation to the anisotropy free energy. Another important basis of our investigation is the connection between the experimentally measured anisotropy constants and the theoretically more fundamental anisotropy coefficients. A significant concept of anisotropy flow is introduced to detect all the possible types of spin-reorientation transitions driven by temperature evolution in the system. Seven types of temperature dependence of the first anisotropy constant and 14 types of spin-reorientation transitions are discovered in this one-sublattice system. Phase diagrams for these temperature behaviors and the spin-reorientation transitions are given by means of analytical and numerical calculations. [S0163-1829(99)05141-3]

I. INTRODUCTION

The single-ion model has gained great success in interpreting the origin of the magnetocrystalline anisotropy in local electron systems, such as rare-earth (RE) ions.[1,2] Rare-earth–transitional-metal compounds are an important class of magnetic materials. Magnetic anisotropy of the compounds is known to originate mainly from the crystal field (CF) acting on the unfilled $4f$ shell of the rare earths. Provided the exchange interaction is dominated, the temperature dependence of the rare-earth contribution to the anisotropy energy could be described analytically on the basis of a linear approximation which takes into account corrections to the first-order thermodynamic perturbation in the crystal field.[3,4] However, the partition function can be calculated exactly only in rare cases or under special unrealistic assumptions. Confined to the low-temperature limit, Zener's $n(n+1)/2$ power law could be established,[5] where $n=2$, 4, 6 is the order of the CF interaction. Within this framework, the temperature dependence of the expectation values of the Stevens' operators is written as power laws of the reduced magnetization. Another important particular case is the $J=\infty$ classical limit where expressions for the temperature dependence of the anisotropy coefficients at arbitrary temperature were obtained by Keffer[6] and further discussed by Callen and Callen.[7] In this case, the hyperbolic Bessel function and its inversion are implemented to calculate the temperature dependence of the single-ion anisotropy. Compared with each other, these two methods have individual advantages and disadvantages. The former can be applied for any value of J, but effective only in the case of $T \ll T_c$. The latter can be applied for arbitrary T, but only in the case of $J=\infty$.

Recently, Millev *et al.*[8,9] successfully applied a simple parametric method to the Callen and Shtrikman theory of magnetic single-ion anisotropy,[10] as has already been corroborated to be feasible within the frameworks of the mean-field (MF) approximation and the random-phase approximation.[9] The salient feature of this parametric method is that the exact thermal averages of the Setevens' operators could be given out for arbitrary T and any value of J, without any confinement or assumption only needs to sweep the generalized effective field between zero and infinity.[11–14] As a result, the temperature dependence of the single-ion anisotropy could be precisely calculated without recourse to rough iteration,[11,12] then the spontaneous spin-reorientation transition (SRT) driven by temperature could be studied in detail by using the concept of anisotropy flow.[13,14] In Ref. 13, a general discussion of the temperature dependence of the magnetic single-ion anisotropy and anisotropy-flow diagrams in the plane (K_1-K_2) were given for both the uniaxial and the cubic cases in the two-constant phenomenological expression for the free energy. As is well known, neglecting the in-plane anisotropy, a complete description of the uniaxial one-sublattice system should be based on the three-constant approximation to the anisotropy free energy.[14] However, so far an exhaustive study on the temperature variation of the uniaxial anisotropy constants within the three-constant approximation is absent. Therefore, this paper aims to carry out a thorough investigation of the temperature behavior of the anisotropy constants by adjusting the intrinsic anisotropy parameter continuously, and detect all the possible SRT's via tracing the evolution of the anisotropy flow in the anisotropy space of a uniaxial one-sublattice system.

The remainder of this paper is arranged as follows. The theoretical framework of the calculating method we used will be described briefly in Sec. II. The temperature dependence of the anisotropy constants and all the possible SRT's in the single-ion one-sublattice system will be presented in Secs. III and IV, respectively. Section V is the summary.

II. THEORETICAL FRAMEWORK

There exist two established ways to characterize the free energy of the magnetocrystalline anisotropy which depends on the orientation of macroscopic magnetization with respect

to the crystallographic axes. One way is to expand the anisotropy energy in symmetry-dictated combinations of powers of direction cosines of magnetization, whereby the description is in terms of the set of the experimentally measured anisotropy constants $\{K_i\}$. Alternatively, one may expand in spherical harmonics and this gives rise to the description in terms of the set of the theoretically more fundamental anisotropy coefficients $\{\bar{\kappa}_n\}$.[15–17] In the uniaxial system, with the assumption of negligible in-plane anisotropy, the anisotropy free energy F_A in the ''constants'' K_i representation is given by

$$F_A=\sum_i K_i \sin^{2i}(\theta), \quad i=1,2,3, \tag{1}$$

where θ is the angle between the direction of magnetization and the crystallographic axis (c axis) of uniaxial symmetry. In the ''coefficients'' representation F_A', which is equivalent to F_A so far as the angular dependence is concerned, is described as

$$F_A'=\sum_n B_n^0 p_n(J) Y_n^0(\theta)\bar{\kappa}_n(T), \quad n=2,4,6, \tag{2}$$

where B_n^0 are the Elliott-Stevens CF parameters,[4,18] $Y_n^0(\theta)$ are the spherical harmonics, and the anisotropy coefficients are defined as the thermal averages of the Setevens' operators $\langle \hat{O}_n^0\rangle(T)$ normalized against their zero-temperature values:[8,15,17]

$$\bar{\kappa}_n(T)\equiv\frac{\langle \hat{O}_n^0\rangle(T)}{\langle \hat{O}_n^0\rangle(0)}. \tag{3}$$

The zero-temperature values $p_n(J)\equiv\langle \hat{O}_n^0\rangle(0)$ are certain J-dependent products:

$$p_2(J)=2J\left(J-\frac{1}{2}\right), \quad J>\frac{1}{2};$$

$$p_4(J)=8J\left(J-\frac{1}{2}\right)(J-1)\left(J-\frac{2}{3}\right), \quad J>\frac{3}{2};$$

$$p_6(J)=16J\left(J-\frac{1}{2}\right)(J-1)\left(J-\frac{3}{2}\right)(J-2)\left(J-\frac{5}{2}\right), \quad J>\frac{5}{2}, \tag{4}$$

where J is the angular momentum quantum number, while the anisotropy coefficients turn out to be linear combination of the moments $M_n\equiv\langle(\hat{J}_z)^n\rangle$,

$$\bar{\kappa}_2=\frac{1}{p_2(J)}[3M_2-J(J+1)],$$

$$\bar{\kappa}_4=\frac{1}{p_4(J)}[35M_4+(25-30J-30J^2)M_2+3J^2(J+1)^2-6J(J+1)],$$

$$\bar{\kappa}_6=\frac{1}{p_6(J)}\{231M_6+[735-315J(J+1)]M_4+[294-525J(J+1)+105J^2(J+1)^2]M_2-60J(J+1)+40J^2(J+1)^2-5J^3(J+1)^3\}, \tag{5}$$

where $\hat{J}_z$ is the z component of the angular momentum operator of a given ion. Fortunately, all the moments M_n and, consequently, all $\bar{\kappa}_n$'s can be expressed via the first moment M_1 or, equivalently, the reduced magnetization $m=M_1/J$. Moreover, the functional dependence $M_n=M_n(M_1)$ itself is model independent in all renormalized quasi-independent collective excitation theories including the spin-wave theory, the random-phase approximation, some improved decoupling schemes in the Green's-function approach,[19,20] and the mean-field theory. One can easily derive all the moments M_n from the moment's generating function $\Omega(\alpha,x)$ by means of n-order partial differentials with respect to α,

$$M_n(x)=\frac{\partial^n}{\partial\alpha^n}\Omega(\alpha,x)\bigg|_{\alpha=0}=\frac{\partial^n}{\partial\alpha^n}\frac{\sinh[(2J+1)/2(\alpha+x)]/\sinh[(\alpha+x)/2]}{\sinh[(2J+1)/2x]/\sinh(x/2)}. \tag{6}$$

The first moment M_1 can be found with $n=1$,

$$M_1(x)=JB_J(Jx), \tag{7}$$

where $B_J(y)$ is the well-known Brillouin function, while x is the generalized effective field relative to the average number $\phi(T)$ of magnetic quasiparticle excitations.[10] Directing our attention to the MF approximation in the zero external field, we can attain a simple expression for x,

$$x=\frac{3}{J+1}\frac{m}{t}, \tag{8}$$

where $t\equiv T/T_C$ and T_C is the MF Curie temperature. Because the temperature part in the generalized effective field is factorized out from the magnetization, a function $t(x)$ can be easily obtained:

$$t=t(x)=\frac{3}{J+1}\frac{m(x)}{x}. \tag{9}$$

Therefore, if x sweeps between 0 and ∞, t will be evaluated from 1 to 0, the left limit being attained for $T\to T_C$, while the right one corresponds to zero temperature. Finally, the explicit temperature dependence of the anisotropy coefficients for any J in the whole temperature range can be computed by using as a parameter the generalized effective field x.[9] The simple parametric method could be summarized as the following formal procedure: Let x sweep between 0 and ∞, compute $M_1(x)$ [i.e., $m(x)$] from Eq. (7), compute t from Eq. (9) by using x and $m(x)$, and finally compute $\bar{\kappa}_2$, $\bar{\kappa}_4$, and $\bar{\kappa}_6$ from Eq. (5) by using $M_2(x)$, $M_4(x)$, and $M_6(x)$ from Eq. (6). Eventually, collect pairs of computed points corresponding to the same value of x to get $\bar{\kappa}_2(t)$, $\bar{\kappa}_4(t)$, and $\bar{\kappa}_6(t)$ or whatever other dependence parametrized by x in which one might be interested.

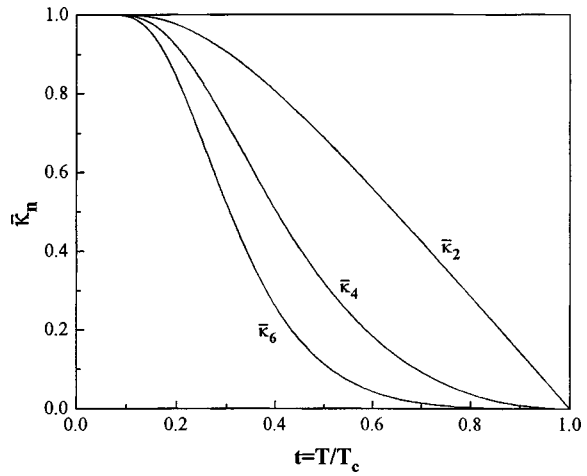

FIG. 1. Magnetic anisotropy coefficients $\bar{\kappa}_2$, $\bar{\kappa}_4$, and $\bar{\kappa}_6$ as functions of reduced temperature $t=T/T_c$ for $J=3$ in the MF approximation.

The relevant information about the experimentally accessible quantities K_i is gained by feeding the information from the calculation of $\bar{\kappa}_n$ into the relations connecting the anisotropy constants K_i with the anisotropy coefficients $\bar{\kappa}_n$ in uniaxial symmetry,[21,22]

$$K_1(t)=\left(K_1^0+\frac{8}{7}K_2^0+\frac{8}{7}K_3^0\right)\bar{\kappa}_2(t)-\frac{8}{7}\left(K_2^0+\frac{18}{11}K_3^0\right)\bar{\kappa}_4(t)+\frac{8}{11}K_3^0\bar{\kappa}_6(t), \tag{10}$$

$$K_2(t)=\left(K_2^0+\frac{18}{11}K_3^0\right)\bar{\kappa}_4(t)-\frac{18}{11}K_3^0\bar{\kappa}_6(t), \tag{11}$$

$$K_3(t)=K_3^0\bar{\kappa}_6(t), \tag{12}$$

where $K_i^0\equiv K_i(t=0)$ are the intrinsic (ground-state) anisotropy constants and associated with the microscopic parameters B_n^0 and $p_n(J)$.[23] Here we concentrate on the single-ion first anisotropy constant K_1 in the one-sublattice system of uniaxial symmetry. It is obvious that the temperature dependence of $K_1(t)$ can be uniquely determined by a set of initial constants (K_1^0,K_2^0,K_3^0), provided J is fixed. In fact, the variation of J does not affect the classification of the types of the temperature dependence of anisotropy constants.[12] So we set $J=3$ in the whole calculation for the sake of brevity. Meanwhile, the temperature dependence of the basis functions $\bar{\kappa}_n$ is solely determined by a given J.[9,13] The temperature curves of the basis functions for $J=3$ are shown in Fig. 1. All the three basis functions are strictly monotonically decreasing functions. $\bar{\kappa}_2$ is convex upwards for all t, while both $\bar{\kappa}_4$ and $\bar{\kappa}_6$ have a typical bell shape and an inflection point. $\bar{\kappa}_6$ falls off much faster than $\bar{\kappa}_2$ and $\bar{\kappa}_4$.

III. TYPES OF TEMPERATURE VARIATION OF K_i

The most attractive part of the temperature dependence is that of the reduced anisotropy constants $\bar{K}_i\equiv K_i/K_i^0$, which always starts from the positive value of unity at $T=0$ to zero at $T=T_c$ regardless of the sign of K_i^0,

$$\bar{K}_1=\left(1+\frac{8}{7}x_0+\frac{8}{7}y_0\right)\bar{\kappa}_2-\frac{8}{7}\left(x_0+\frac{18}{11}y_0\right)\bar{\kappa}_4+\frac{18}{11}y_0\bar{\kappa}_6, \tag{13}$$

$$\bar{K}_2=\left(1+\frac{18}{11}\frac{y_0}{x_0}\right)\bar{\kappa}_4-\frac{18}{11}\frac{y_0}{x_0}\bar{\kappa}_6, \tag{14}$$

$$\bar{K}_3=\bar{\kappa}_6. \tag{15}$$

After normalization, more compact and expressive relations between the constants and coefficients arise, and the temperature variation of the normalized constant $\bar{K}_1$ will only depend on two entirely independent variables $x_0=K_2^0/K_1^0$ and $y_0=K_3^0/K_1^0$, and $\bar{K}_2$ on their ratio $r\equiv y_0/x_0=K_3^0/K_2^0$.

It is interesting to note that the third reduced constant $\bar{K}_3$ has the same temperature dependence as the highest-order coefficient $\bar{\kappa}_6$. Consequently, $K_3(t)$ strictly monotonically decreases (or increases) for $K_3^0>0$ (or $K_3^0<0$) with increasing temperature. The curve always possesses the bell-shape characteristic and an inflection point approximately halfway down from T_c. As far as the *f*-electron one-ion anisotropy, there is no gainsay that the temperature dependence of the third constant in uniaxial symmetry as well as that of the second constant in cubic symmetry could be completely described through the highest-order coefficient.[13]

Both the fourth- and sixth-order basis functions enter into the expression of $\bar{K}_2(t)$ which has no business with the lowest-order basis function. In this case when only two basis functions of $\bar{\kappa}_n$ are involved in a linear superposition of the kind given in Eq. (14), it turns out possible to carry out an explicit and conclusive analytical classification of the allowed types of temperature behavior $\bar{K}_2(t)$, which is valid beyond the MF approximation.[13] In doing so, one needs to investigate the signs of the first derivative of $\bar{K}_2$ with respect to t at both ends of variation, i.e., for $t\to 0$ $(T\to 0)$ and $t\to 1$ $(T\to T_c)$. Taking advantage of the assumptions and the asymptotic of the coefficients $\bar{\kappa}_n$ in these two limits as in Ref. 13, one then finds the possible classification of the types of variation by exhausting the allowed combination of the signs of the first derivative. Three generic types of variation of $K_2(t)$ are possible depending on the ratio of the intrinsic constants K_3^0 and K_2^0 only:

(I) For $r>5/9$, $K_2(t)$ has an extremum which is a minimum or a maximum depending on the sign of K_2^0.

(II) For $-11/18<r<5/9$, $K_2(t)$ is strictly monotonically decreasing and increasing for $K_2^0>0$ or $K_2^0<0$, respectively.

(III) For $r<-11/18$, $K_2(t)$ has a zero point at a certain temperature between zero and Curie temperature.

The classification is consistent with that of the canonic dependence of $K_2(m)$ on magnetization[12] which is valid for the whole class of Callen and Shtrikman.[10] It is essentially due to the monotonic behavior of magnetization with temperature and the invariance of the sign of $dm/dT<0$ in the whole range. Additionally, the consistence demonstrates that the above classification is also generally effective for the whole class theories envisaged.[10] Figure 2 gives some representative curves for $\bar{K}_2(t)$ calculated in the MF approximation. The borderlines between the different regimes are drawn with thick lines. All the curves in the monotonic re-

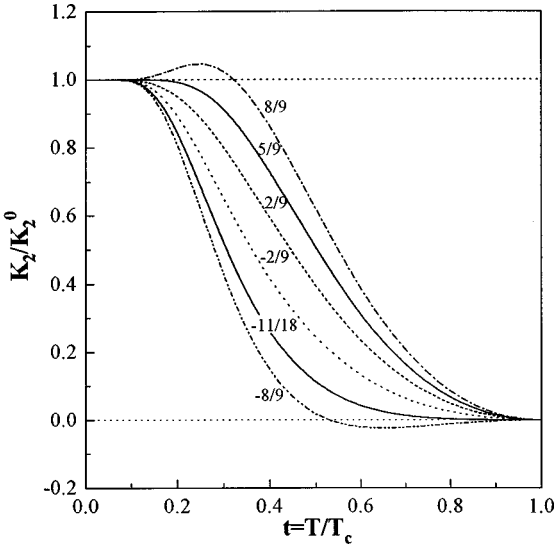

FIG. 2. The anisotropy constant $K_2(t)$ as normalized against its zero-temperature value K_2^0 in the MF approximation for some typifying ratio of $r=K_3^0/K_2^0$. The value of r is given next to each curve. Thick lines denote the borderlines between the three detected regimes of variation.

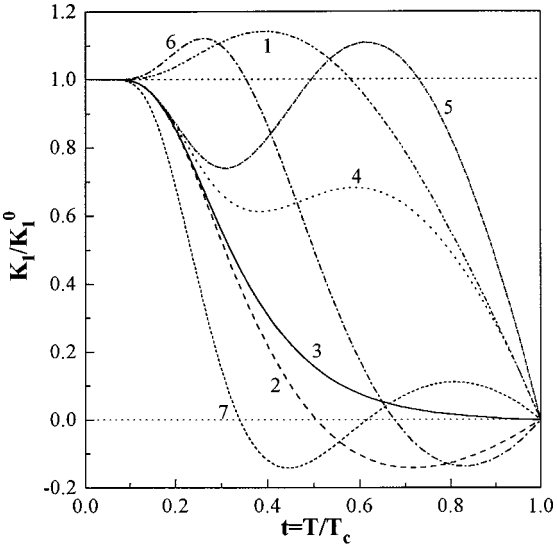

FIG. 3. The anisotropy constant $K_1(t)$ as normalized against its zero-temperature value K_1^0 in the MF approximation for some typifying initial parameters (x_0,y_0). The parameters used during the calculations are (1) (1.0, −0.05); (2) (−2.0, 0.6); (3) (−2.0, 1.15); (4) (−2.0, 3.0); (5) (−2.0, 4.3); (6) (2.0, −3.8); (7) (−5.0, 4.8).

gimes inherit the characteristic of the basis functions, i.e., the bell shape and an inflection point.

At last, we come to the most complicated case of $\overline{K}_1(t)$ which contains three basis functions and two independent variables x_0 and y_0. In this case, it does not seem possible to require an analytic exhaustion of the possible types of variation of $\overline{K}_1(t)$, since the first derivatives of $\overline{K}_1$ with respect to t at both ends are insufficient to detect all existing types.[14] Now, the only way is to have recourse to the numerical calculation in the MF approximation by implementing the specific parameter method. Hence a self-suggesting procedure would be used to study numerically all possible values in the initial parametric space (x_0-y_0) and to see what types of temperature behavior one gets for $\overline{K}_1(t)$. As shown in Fig. 3, one can gain seven different types of temperature behavior for $\overline{K}_1(t)$ after performing the above procedure and exhausting the initial parameters. We are familiar with the former three types (see curves 1–3 in Fig. 3) which possesses the features of one extremum, one zero-point, and monotonic variation, respectively. These features can be easily realized and distinguished through the combination of two basis functions. An unexpected feature of two internal extrema emerges on the latter four types (see curves 4–7 in Fig. 3). Especially, the first anisotropy constant $\overline{K}_1$ exhibits two zero points (changes its sign twice) for realistic values of the constitutional parameters in the case of the seventh types. The sixth type has two extrema and one zero point, while no zero point can be find for the types 4 and 5. Besides, in the case of the fifth type the $\overline{K}_1(t)$ decreases first, increases after reaching a minimum, then decreases again after arriving at a maximum whose value is even greater than unity at $t=0$. The only discrepancy between the fourth and fifth types is that the second extremum locates below or above the dashed line denoting unity. No more peculiar variation can be detected again, which agrees well with a general theorem by virtue of which the linear superposition of p functions satisfying certain conditions may not have more than $p-1$ zeros or internal extrema on a bounded interval.[14]

Up to now, an interesting problem, how to classify those types in the initial parametric space (x_0,y_0), arises. This can be solved by applying the first derivative of $\overline{K}_1(t)$ at both ends of the interval of variation and by numerical calculation probing the anisotropy space systematically. The result is summarized in Fig. 4 where six regions are separated for the above seven types of temperature dependence of $\overline{K}_1(t)$. We merge types 4 and 5 into one region since their shapes seem

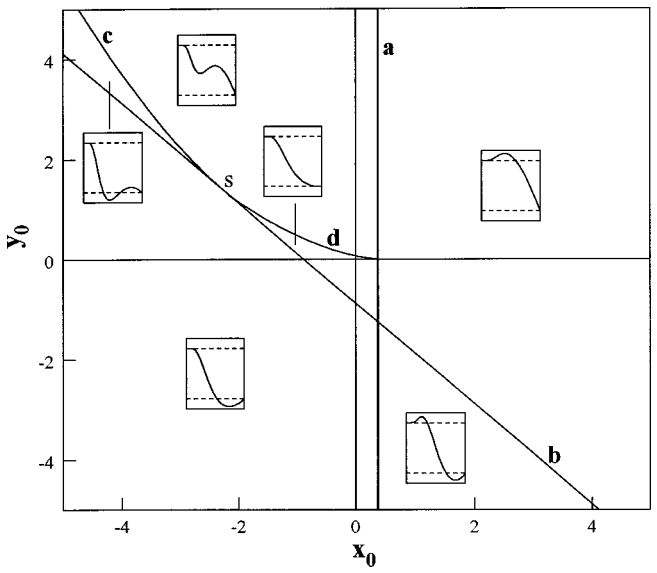

FIG. 4. Phase diagram for different types of temperature dependence of the reduced anisotropy constant $\overline{K}_1(t)$ in the initial parameter space (x_0-y_0). The equations of lines a and b are $x_0-\frac{3}{8}=0$ and $1+\frac{8}{7}x_0+\frac{8}{7}y_0=0$, respectively. Curves c and d are numerically calculated in the MF approximation. The point s is the common crosspoint between the line b and the curves c and d.

like each other. The borderlines between different regions are drawn with thick lines. Lines *a* and *b* are determined from analyzing the sign of $\partial\overline{K_1}/\partial t$ for $t\to 0$ and $t\to 1$, respectively. It turns out that the sign of $\partial\overline{K_1}/\partial t$ for $t\to 0$ is the same as the sign of the expression

$$S_0 = x_0 - \frac{3}{8}, \tag{16}$$

while the sign of $\partial\overline{K_1}/\partial t$ for $t\to 1$ is given by the sign of the expression

$$S_1 = -\left(1 + \frac{8}{7}x_0 + \frac{8}{7}y_0\right). \tag{17}$$

The expression in the bracket of Eq. (17) is the same as the coefficient before the basis function $\overline{\kappa_2}$ in Eq. (13). This indicates that the temperature behavior of the single-ion anisotropy at high temperatures is dominated by the lowest-order coefficient, because of the much faster decline of the higher-order ones at high temperatures. Four regions can be separated by lines *a* ($x_0-\frac{3}{8}=0$) and *b* ($1+\frac{8}{7}x_0+\frac{8}{7}y_0=0$) in the initial parametric space (x_0-y_0):

(I) $x_0-\frac{3}{8}>0$ and $1+\frac{8}{7}x_0+\frac{8}{7}y_0>0$, for type 1;

(II) $x_0-\frac{3}{8}>0$ and $1+\frac{8}{7}x_0+\frac{8}{7}y_0<0$, for type 6;

(III) $x_0-\frac{3}{8}<0$ and $1+\frac{8}{7}x_0+\frac{8}{7}y_0<0$, for type 2;

(IV) $x_0-\frac{3}{8}<0$ and $1+\frac{8}{7}x_0+\frac{8}{7}y_0>0$, for types 3, 7, 4 and 5.

With the aid of numerical calculation, curves *c* and *d* can be delineated in region IV to distinguish types 7 and 3 from 4 and 5, respectively. One cannot find an analytical form for the curves *c* and *d* because there is no way to get the first derivative of $\overline{K_1}(t)$ at arbitrary temperature. It is worth noting that line *b* and curves *c* and *d* cross over a common point *s* (−9/4, 11/8). Putting the coordinates of point *s* into Eqs. (13) and (14), one will get a surprising result that both $\overline{K_1}$ and $\overline{K_2}$ have the same temperature behavior as $\overline{K_3}$, i.e., the temperature behavior of the basis function $\overline{\kappa_6}$. As for the points on the curve *c*, only one zero point just corresponding to the first extremum appears in the temperature dependence of $\overline{K_1}$. Under this condition, a slight decrease of x_0 or y_0 will bring about two zero points, while a slight increase will make the zero point vanish.

So far, all the possible types of temperature variation of $\overline{K_1}$ have been thoroughly studied with the three-constant approximation to the anisotropy free energy. One conclusive point could be drawn from the above discussion that variation of the intrinsic parameters x_0 and y_0 versifies the temperature behavior of the constants of single-ion uniaxial anisotropy.

IV. SPIN-REORIENTATION TRANSITION

In the one-sublattice model, the temperature-driven SRT is mainly induced by the competition between the anisotropy coefficients of different orders. However, the variation of the intrinsic anisotropy parameters x_0 and y_0 can adjust their competition and give rise to many different kinds of temperature behavior of the anisotropy constants as described in the preceding section. Hence, various procedures of SRT's would be expected. Therefore, it would be very meaningful to probe all the possible SRT's in the initial parameter space (x_0-y_0). It is well known that the magnetic phase diagrams for easy magnetization directions (EMD's) depend on the sign of the first anisotropy constant K_1.[24] So we will analyze the phase diagrams for the SRT relevant to different signs of K_1^0.

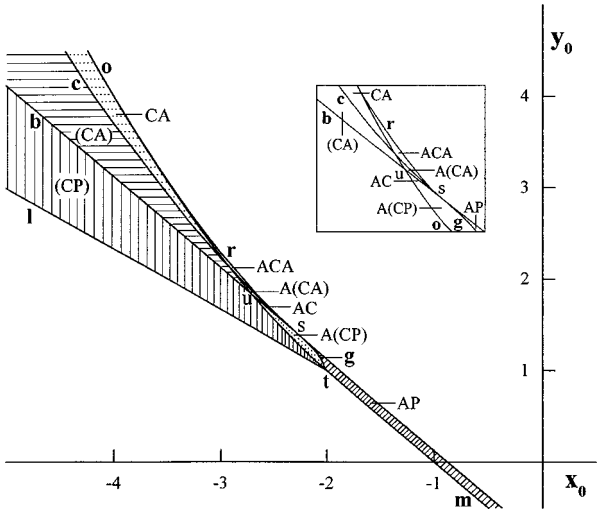

FIG. 5. Phase diagram for different kinds of SRT's in the initial parameter space (x_0-y_0) with $K_1^0>0$. Curve *o* and lines *l* and *m* are the borderlines between three thermodynamically stable phases in zero temperature. Curves *c* and line *b* are the same as in Fig. 4, curves *g* and *r* are numerically determined in the MF approximation. The configurations of different regions around point *u* are schematically represented in the inset.

Before beginning our work, it is worth introducing an important concept of anisotropy flow recently developed by Millev *et al.*[13,14] The anisotropy flow means a specific trajectory in the parameter space $[x(T)-y(T)]$, along which the system evolves from $T=0$ to T_c with increasing temperature. The trajectory starts from the initial point (x_0,y_0) and usually flows into the origin at $T=T_c$. It is then quite possible that at some values of temperature which depend on the initial condition at zero temperature, this trajectory crosses over to some neighboring regions stabilizing other EMD's. Accordingly, at some particular temperatures the EMD has to switch to a new direction so that a transition related with spin reorientation happens. The initial condition (x_0,y_0) is of exceptional importance. Given this pair, the temperature flow of the anisotropy is deterministic within the MF approximation. Hence the existence and the type of crossover are determined solely by the initial condition. So we are in a position to detect all such crossovers and peculiarities in great detail with the aid of the concept of the anisotropy flow.

A. $K_1^0>0$

Supposing the sign of K_1^0 is positive, we investigate the anisotropy flow in the plane $[x(T)-y(T)]$ for all the possible initial points (x_0,y_0). Eight types of SRT's [(CP), A(CP), AP, AC, (CA), CA, A(CA), ACA] are detected and the phase diagram concerning the conditions of their existences is summarized in Fig. 5, where curve *o* ($x_0^2-4y_0=0$) and lines *l* ($2x_0+3y_0+1=0$) and *m* ($x_0+y_0+1=0$)

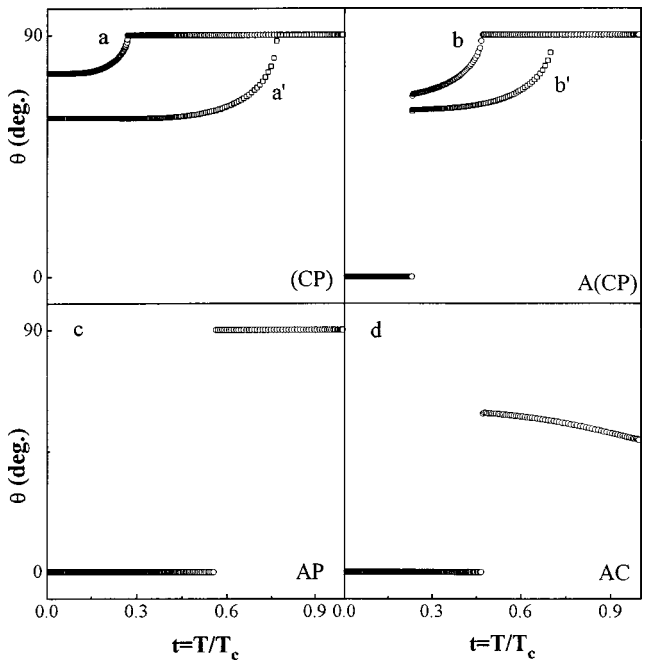

FIG. 6. Temperature variation of the angle of EMD with respect to the c axis during some typifying processes of SRT's in the case of $K_1^0>0$. The initial parameters used during the calculation are (a) $(-3.0, 1.75)$; (a′) $(-4.0, 3.0)$; (b) $(-2.3, 1.35)$; (b′) $(-2.5, 1.59)$; (c) $(-1.7, 0.8)$; (d) $(-2.4, 1.525)$.

are the borderlines between three thermodynamically stable phases, i.e., easy-axis (A), easy-plane (P), and easy-cone (C) at zero temperature. Line b and curve c are the same as in Fig. 4. The phase diagram is divided into two parts by line b: $1+\frac{8}{7}x_0+\frac{8}{7}y_0=0$. For the part above line b, the system will have easy-axis anisotropy at high temperature, and for the part below it, the high-temperature state is easy plane. Next, we deal with the different SRT's corresponding to the different zones in Fig. 5.

(CP). At low temperature, the magnetic moment prefers a conical orientation as a result of the competition between the high- and low-order anisotropy coefficients. With increasing temperature, the high-order anisotropy coefficients decrease faster than the low-order anisotropy coefficient, so that at high temperatures the EMD is mainly determined by the latter. The EMD will gradually change toward the plane, as shown in Figs. 6 (a) and (a'). Here, we denote this kind of SRT as (CP), where C and P indicate cone and plane, respectively, and brackets indicate a continuous process. The anisotropy flows of a and a' are shown in Fig. 8, both of them consist of two pieces $a1$ and $a2$, $a'1$ and $a'2$, respectively. This feature is intimately connected with the number of zeroes of K_1. As K_1 tends to zero, the trajectory goes to infinity in the chosen standard presentation and, following the change of the sign of K_1, reemerges in another section of the parameter space. Therefore, the trajectory will be cut into $n+1$ pieces when K_1 has n zeroes. Tacking down the trajectories a and a', one can find that the SRT's occur before the variance of the sign of K_1 for the case of a, and after for a'. This demonstrates that the SRT of (CP) is not induced by the change of the sign of K_1, but by the crossover of its anisotropy flow with the borderline l in the parameter space $(x-y)$.

A(CP). There are two minima for the anisotropy energy at low temperatures, one along the c axis and the other along a conical direction. The former is the lowest at low temperatures, but the latter becomes lower with increasing temperature and gives rise to a first-order SRT from the c axis to a conical direction. After the discontinuous transition, the easy direction will gradually change from the conical direction to the basal plane [see Figs 6(b) and 6 (b')]. The first discontinuous SRT happens at the crosspoints where the trajectory b and b' cross the dotted curve o (in Fig. 8). The two minima in the anisotropy energy become equivalent at the crosspoint. The following continuous transitions in b and b' have the same features as transitions in the above cases of a and a'.

AP. In this case, both the c axis and the direction perpendicular to the c axis are minima for the anisotropy energy. The magnetic moment favors axial orientation at low temperatures and planar at high temperatures. At T_s, the EMD changes from axial to planar direction through a first-order transition as shown in Fig. 6(c), whose anisotropy flow crosses the borderline m in Fig. 8. The curve g between points s and t in Fig. 5 is the borderline between A(CP) and AP. It can be numerically determined by the parametric method, since the anisotropy flow starting from every point on it has to pass through the common crosspoint t between borderlines in Fig. 8. If one takes Zener's power law to approximate the temperature dependence of the basis functions $\overline{\kappa_n}$, an equation satisfied by curve g can be obtained,

$$4^{18}y_0^7(7+8x_0+8y_0)^{11}+(11x_0+18y_0)^{18}=0. \qquad (18)$$

AC. The region for this kind of SRT is only a segment of line b between points u and s. The anisotropy flow starting from the point (excluding s) on line b has a straight trajectory along the line b, and finally evolves to a specific points $(-7/8, 0)$ not the origin in the planes $(x-y)$ for $K_1>0$ or $K_1<0$. This is because the condition $1+\frac{8}{7}x+\frac{8}{7}y=0$ is always satisfied by the system at any temperature. Making s as the initial point, no anisotropy flow can be formed since all the anisotropy constants have the same temperature behavior. The transition d in Fig. 6 shows a first-order transition AC which takes place when its straight trajectory crosses the dotted curve o [Fig. 8 (d)]. The limitation of the conical angle is 49.1° before the magnetism vanishes.

(CA), CA. The SRT of (CA) [Fig. 7 (e)] is a continuous process, while CA [Fig. 7 (f)] is a discontinuous one. The curve c defined in Fig. 4 separates them from each other. According to the knowledge in Fig. 4, one knows that the trajectory e in Fig. 8 comprises three pieces ($e1$-$e2$-$e3$). The transition temperature T_s is just corresponding to the second zero of K_1. However, the trajectory f has only one piece in the plane $K_1>0$ since K_1 does not change its sign in the whole process. The first-order transition CA takes place at the crosspoint between its trajectory f and the dotted curve o.

A(CA),ACA. Extending the regions of (*CA*) and *CA* to point s, one can obtain two regions for *A*(*CA*) and *ACA*, respectively. As shown in Figs. 7(g) and 7(h), a first-order transition *AC* is added before (*CA*) and *CA*. Curve r is numerically calculated within the MF approximation. From their anisotropy flows in Fig. 8, the first discontinuous transition is induced by the crossover with the dotted curve o, the

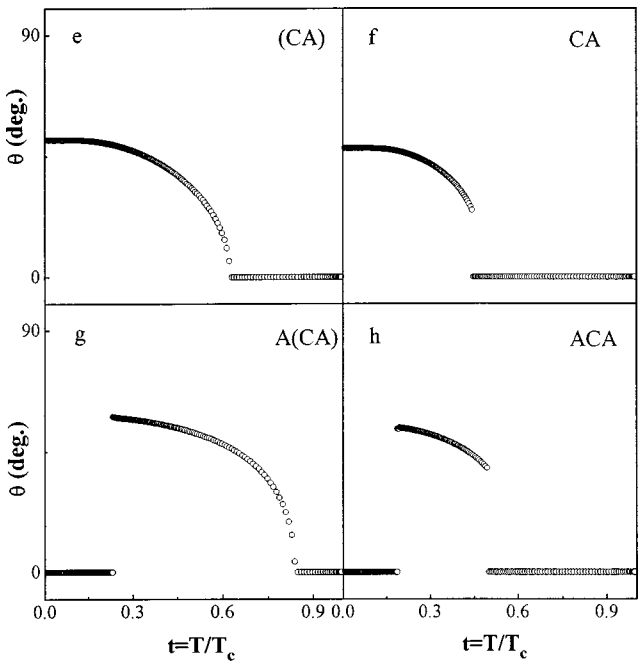

FIG. 7. Temperature variation of the angle of EMD with respect to the *c* axis during some typifying processes of SRT's in the case of $K_1^0>0$. The initial parameters used during the calculation are (e) $(-4.0, 3.5)$; (f) $(-4.0, 3.75)$; (g) $(-2.7, 1.85)$; (h) $(-3.0, 2.262)$.

second transition is induced by the second variation of the sign of K_1 for *g* and by the crossover again with the dotted curve *o* for *h*.

In the remaining region no other SRT could be detected, the low-temperature state holds at high temperatures. It is thus clear that the different phases as defined by thermodynamic minimization are of different relative stability under variation of temperature. The easy-plane phase is the most stable in this sense and a system starting at $T=0$ from within this phase never leaves it. The *c*-axis phase is of intermediate stability. The titled-axis phase is the most unstable in the sense that systems starting their temperature evolution from within this phase always run away to other neighboring phases.

B. $K_1^0<0$

Changing the sign of K_1^0, not only the magnetic phase diagram at zero temperature is varied, but also the competition between the anisotropy coefficients of different order. Therefore, different kinds of SRT's and different conditions of their existences are expected in the initial plane $(x_0 - y_0)$. The result is shown in Fig. 9, where curve o' $(x_0^2 - 2x_0y_0 - 4y_0 - 3y_0^2 = 0)$ and line l $(2x_0 + 3y_0 + 1 = 0)$ are borderlines between easy-cone and easy-plane phases. At zero temperature, the easy-axis phase is unable to be stabilized, provided $K_1^0<0$. Line b $(1 + \frac{8}{7}x_0 + \frac{8}{7}y_0 = 0)$ also cuts the phase diagram into halves, the high-temperature state is easy-plane for the upper part, and easy-axis for the lower. Eight types of SRT's $[(CA), P(CA), PA, CPA, (CP), CP, PAP, CPAP]$ are discovered after a systematic investigation on the anisotropy flow for any initial parameter (x_0, y_0). Some typical transitions representative of every kind of SRT

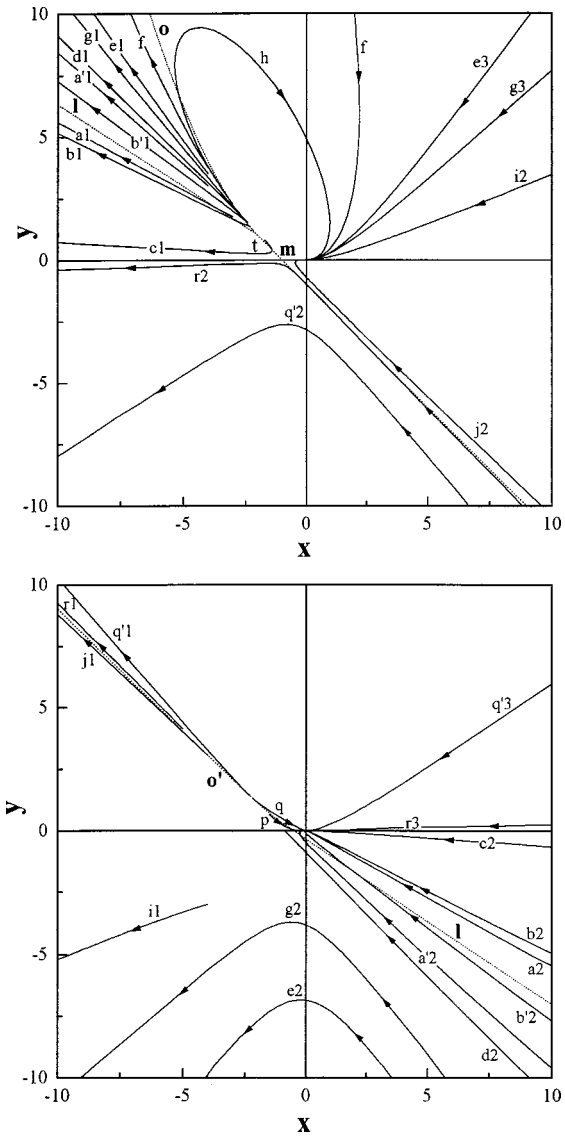

FIG. 8. Anisotropy flows in the plane $(x-y)$ for these typifying processes of SRT's shown in Figs. 6, 7, 10, and 11. Dotted lines $l(2x+3y+1=0)$ and $m(x+y+1=0)$ and curves $o(x^2-4y=0)$ and $o'(x^2-2xy-4y-3y^2=0)$ are borderlines between the three thermodynamically stable phases at arbitrary temperature. The upper plane corresponds to $K_1>0$, the lower one to $K_1<0$. The arrows indicate the direction of temperature evolution as T increases from zero to T_c.

are exhibited in Figs. 10 and 11, and some relevant anisotropy flows could be found in Fig. 8 by looking for the same notation.

(*CA*) is a continuous transition whose region is largest. The variation of the sign of K_1 gives rise to this transition [Fig. 8(i)]. A first-order transition from the basal plane to a certain conical angle is expected to take place before (*CA*) when the initial point locates in the region below the line *b* and above the curve o'. The trajectory *j* in Fig. 8 realizes the transition of $P(CA)$ in expectation, it crosses the dotted curve o' before going toward infinity.

Two types of SRT's are found on the line *b*, one is *PA*, the other *CPA*. The temperature variation of K_1 has one zero point when the initial point is on the left side of point *s*. It is this zero point that leads to the first-order transition *PA*.

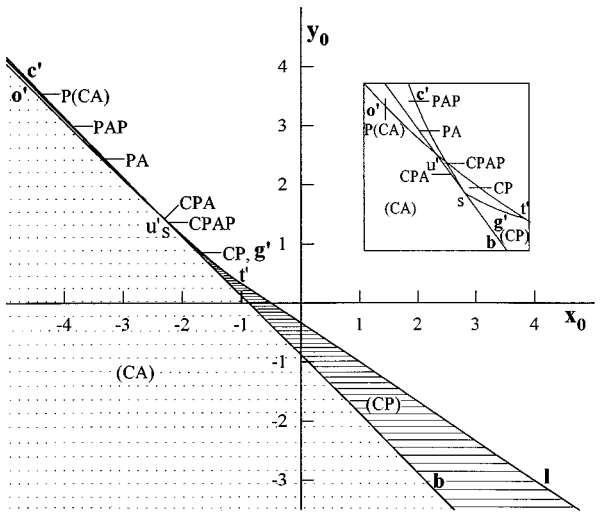

FIG. 9. Phase diagram for different kinds of SRT's in the initial parameter space (x_0-y_0) with $K_1^0<0$. Curve o' and line l are the borderlines between easy-plane and easy-cone stable phases in zero temperature. Line b is the same as in Fig. 4, curves c' and g' are numerically determined in the MF approximation. The configurations of different regions around the point u' are schematically represented in the inset.

However, the low-temperature stable state is easy cone on the line segment of u's, so another first-order transition *CP* will inevitably occur in front of *PA*. Hence the point u' separates these two regions corresponding to *PA* and *CPA*, respectively.

The discrepancy between (*CP*) and *CP* is that the transition is continuous or not. The continuous transition (*CP*) takes place on the crossover between its anisotropy flow with

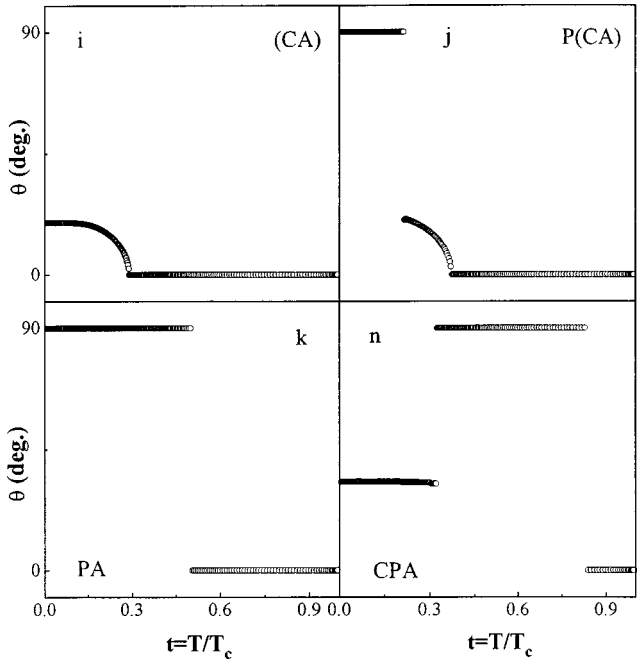

FIG. 10. Temperature variation of the angle of EMD with respect to the c axis during some typifying processes of SRT's in the case of $K_1^0<0$. The initial parameters used during the calculation are (i) $(-4.0, -3.0)$; (j) $(-4.0, 3.08)$; (k) $(-3.0, 2.125)$; (n) $(-2.35, 1.475)$.

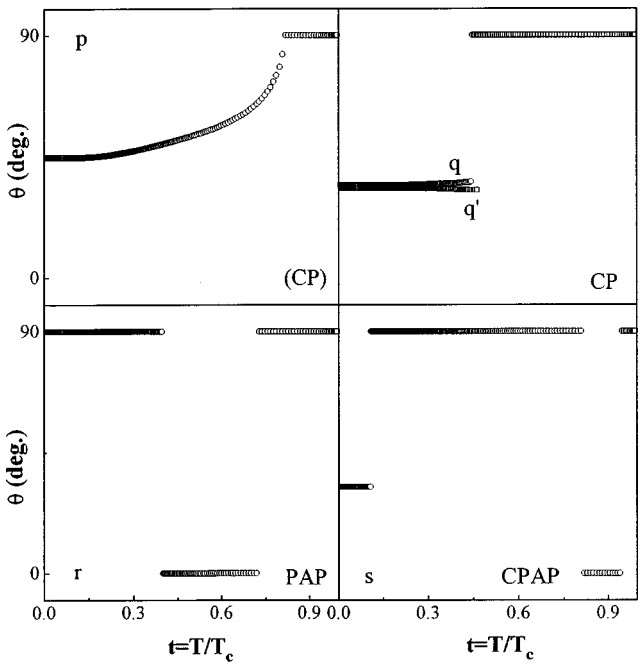

FIG. 11. Temperature variation of the angle of EMD with respect to the c axis during some typifying processes of SRT's in the case of $K_1^0<0$. The initial parameters used during the calculation are (p) $(-1.5, 0.66)$; (q) $(-2.2, 1.33)$; (q′) $(-2.3, 1.4253)$; (r) $(-5.0, 4.16)$; (s) $(-2.4, 1.5253)$.

the dotted line l, while the discontinuous one *CP* with the dotted curve o'. In the region *CP*, the initial point very close to the curve c' develops its anisotropy flow through three pieces, for example $q'1$-$q'2$-$q'3$ in Fig. 8. This results from the variation of the sign of K_1 twice, but both of them do not induce the SRT. The curve g' connecting points s and t' is the boundary between regions (*CP*) and *CP*. It can be numerically calculated by collecting all the initial points whose anisotropy evolution flows through the crosspoint between the dotted line l and curve o' in Fig. 8. Within the framework of Zener's power law, the equation satisfied by the curve g' can be deduced as

$$3^{11}15^7y_0^7(7+8x_0+8y_0)^{11}-(11x_0+18y_0)^{18}=0. \quad (19)$$

The curve c' starting from point s is also numerically determined. Combining line b with curve o' constructs two regions for transitions *PAP* and *CPAP*, respectively. Two discontinuous transitions in *PAP* take place in the plane $K_1>0$, i.e., two crossovers with the dotted borderline m (see the trajectory r in Fig. 8). Moreover, the transition *CPAP* undergoes a much more unusual procedure, that is, three successive first-order reorientation transitions of the easy axis of magnetization. The region for *CPAP* is a very small wedge circled with the line b and curves o' and c', as shown in the inset in Fig. 9. The condition to reproduce the transition *CPAP* is very harsh, any tiny deviation (greater than 0.001) in the initial point shall destroy this reorientation transition. Therefore, it seems rather improbable to observe this kind of SRT in real materials, but it does theoretically exist. No transition in *PAP* and *CPAP* corresponds to the zero point of K_1, although K_1 has two zero points in these two regions. This

clearly demonstrates that one cannot judge the reorientation transition only from the variation of the sign of K_1.

Within the framework of the MF approximation, a one-sublattice system with uniaxial single-ion anisotropy possesses 14 different types of SRT's. Suppose $K_3^0=0$, only three kinds can be found. This indicates that the highest-order anisotropy coefficient plays a very important role in determining the temperature behavior of the system, especially when it is comparable with the low-order anisotropy coefficients. Therefore, it is very significant to systematically study the temperature behavior of the system within the three-constant approximation to the anisotropy free energy.

V. SUMMARY

We have systematically investigated the possible types of temperature dependence of the single-ion anisotropy constants in the uniaxial one-sublattice system within the three-constant approximation to the anisotropy free energy. The analysis has been based on the general relation between the anisotropy constants K_i and coefficients $\overline{\kappa_n}$, when the latter serves as base functions spanning the temperature dependence of anisotropy free energy. A powerful parameter method has been used to calculate the temperature behavior of the system in the MF approximation. The analysis of the anisotropy flow has enabled us to determine regions relevant to the possible types of SRT's in the intrinsic parameter spaces (x_0-y_0) for $K_1^0>0$ and $K_1^0<0$. Seven types of temperature variation of the first anisotropy constant K_1 and 14 types of SRT's have been uncovered in the system on the basis of the first-order statistical-mechanical treatment of the single-ion anisotropy. Prototype materials to which our analysis is immediately applicable are those in which the single-ion contribution comes from RE ions such as RE metals or RE–transition-metal compounds, where the magnetism arising from the transition metal can be neglected, for example, R_3Co, R_3Ni, R_4Co_3, RNi$_5$, RMn$_2$, and so on.[25]

ACKNOWLEDGMENTS

This work has been supported by Project No. 59725103 of the National Sciences Foundation of China and by the Science and Technology Commission of Shenyang and Liaoning.

[1] K. A. Mcewen, in *Handbook on the Physics and Chemistry of Rare Earths*, edited by K. A. Gschneidner, Jr. and L. Eyring (North-Holland, Amsterdam, 1978), Vol. 1, p. 411.
[2] J. Jensen and A. R. Mackintosh, *Rare Earth Magnetism: Structures and Excitations* (Clarendon, Oxford, 1991).
[3] K. H. W. Stevens, in *Magnetism*, edited by G. Rado and H. Suhl (Academic, London, 1963), Vol. 1, pp. 1–24.
[4] M. T. Hutchings, in *Solid State Physics: Advances in Research and Applications*, edited by F. Seitz and D. Turnbull (Academic, New York, 1964), Vol. 16, pp. 227–275.
[5] C. Zener, Phys. Rev. **96**, 1335 (1954).
[6] F. Keffer, Phys. Rev. **100**, 1692 (1955).
[7] H. B. Callen and E. Callen, J. Phys. Chem. Solids **27**, 1271 (1966).
[8] Y. Millev and M. Fähnle, J. Magn. Magn. Mater. **135**, 285 (1994).
[9] Y. Millev and M. Fähnle, Phys. Rev. B **51**, 2937 (1995).
[10] H. Callen and S. Shtrikman, Solid State Commun. **3**, 5 (1965).
[11] Y. Millev, and M. Fähnle, J. Phys.: Condens. Matter **7**, 6909 (1995).
[12] Y. Millev and M. Fähnle, J. Magn. Magn. Mater. **163**, L264 (1996).
[13] Y. Millev and M. Fähnle, Phys. Rev. B **52**, 4336 (1995).
[14] Y. Millev and and M. Fähnle, IEEE Trans. Magn. **MAG-32**, 4743 (1996).
[15] E. Callen and H. B. Callen, Phys. Rev. **139**, A455 (1965).
[16] P. R. Briss, in *Symmetry and Magnetism*, Selected Topics in Solid State Physics, Vol. III, edited by E. P. Wohlfarth (North-Holland, Amsterdam, 1966), pp. 153–181.
[17] M. I. Darby and E. D. Isaac, IEEE Trans. Magn. **MAG-10**, 259 (1974).
[18] R. J. Elliott, in *Magnetic Properties of Rare-Earth Metals*, edited by R. J. Elliott (Plenum, New York, 1972), Chap. I, pp. 1–16.
[19] H. B. Callen, Phys. Rev. **130**, 890 (1963).
[20] R. A. Tahir-Kheli, in *Phase Transitions and Critical Phenomena*, edited by C. Domb and M. S. Green (Academic, London, 1975), Vol. 5B, pp. 259–341.
[21] G. Asti, in *Ferromagnetic Materials*, edited by K. H. J. Buschow and E. P. Wohlfarth (Elsevier, Amsterdam, 1990), Vol. 5, pp. 398–464.
[22] K. H. J. Buschow, Rep. Prog. Phys. **54**, 1123 (1991).
[23] E. R. Callen and H. R. Callen, J. Phys. Chem. Solids **16**, 310 (1960).
[24] G. Asti and F. Bolzoni, J. Magn. Magn. Mater. **20**, 29 (1980).
[25] K. H. J. Buschow, Rep. Prog. Phys. **40**, 1179 (1977).